arXiv:1212.1193v1 [cond-mat.quant-gas] 5 Dec 2012

Quadrature interferometry for nonequilibrium ultracold bosons in optical lattices

E. Tiesinga
Joint Quantum Institute, National Institute of Standards and Technology and University of Maryland,
100 Bureau Drive, Stop 8423 Gaithersburg, Maryland 20899-8423, USA

P. R. Johnson
Department of Physics, American University, Washington DC 20016, USA

(Dated: December 7, 2012)

We develop an interferometric technique for making time-resolved measurements of field-quadrature operators for nonequilibrium ultracold bosons in optical lattices. The technique exploits the internal state structure of magnetic atoms to create two subsystems of atoms in different spin states and lattice sites. A Feshbach resonance turns off atom-atom interactions in one spin subsystem, making it a well-characterized reference state, while atoms in the other subsystem undergo nonequilibrium dynamics for a variable hold time. Interfering the subsystems via a second beam-splitting operation, time-resolved quadrature measurements on the interacting atoms are obtained by detecting relative spin populations. The technique can provide quadrature measurements for a variety of Hamiltonians and lattice geometries (e.g., cubic, honeycomb, superlattices), including systems with tunneling, spin-orbit couplings using artificial gauge fields, and higher-band effects. Analyzing the special case of a deep lattice with negligible tunneling, we obtain the time evolution of both quadrature observables and their fluctuations. As a second application, we show that the interferometer can be used to measure atom-atom interaction strengths with super-Heisenberg scaling $\bar{n}^{-3/2}$ in the mean number of atoms per lattice site, and standard quantum limit scaling $M^{-1/2}$ in the number of lattice sites. In our analysis, we require $M \gg 1$ and for realistic systems $\bar{n}$ is small, and therefore the scaling in total atom number $N = \bar{n}M$ is below the Heisenberg limit; nevertheless, measurements testing the scaling behaviors for interaction-based quantum metrologies should be possible in this system.

PACS numbers: 37.10.Jk, 37.25.+k, 67.85.Hj, 06.20.Dk

Ultracold atoms in optical lattices [1–3] are versatile systems for studying nonequilibrium physics [4–11], particularly for making time-resolved measurements of system observables. For example, lattice collapse-and-revival experiments [4, 12–14] follow atom populations in the $k = 0$ quasi-momentum of nonequilibrium Bose gases versus system evolution time. Our goal is to extend the power of these experiments to enable time-resolved measurements of a greater variety of system observables and Hamiltonians. A second goal is to use nonequilibrium collapse-and-revival dynamics to investigate the physics of interaction-based (or nonlinear) quantum metrology, which exploits multibody dynamics to characterize a system and its parameters [15–22].

In this Letter, we design an interaction-based interferometer for making time-resolved measurements of quadrature operators [23] of nonequilibrium matter fields in optical lattices. Measurement of quantum-field quadratures $X_k = (e^{-i\zeta_k} A_k + e^{i\zeta_k} A_k^\dagger)/2$, where A_k annihilates atoms with quasi-momentum k and spin state a, and ζ_k is a tunable phase, can provide direct determination of the order parameter for a Bose gas [24], as opposed to inferring it from density measurements [25, 26]. The technique, analogous to homodyne detection, works as follows. Exploiting the internal state structure of ultracold atoms, we split a superfluid into two subsystems–the arms of the interferometer–consisting of atoms in different spin states and lattice sites. A Feshbach resonance [27] turns off atom-atom interactions in one spin subsystem, making it a well-characterized reference "beam", while atoms in the other subsystem undergo nonequilibrium dynamics for a variable hold time. Interfering the subsystems via a second beam-splitting operation, spatial quadrature observables are obtained by measuring spin populations.

As a second, distinct application of the interferometer, we show that atom-atom interaction strengths can be determined from the frequencies of matter-wave collapse-and-revival oscillations with "super-Heisenberg" [15–18] scaling $\bar{n}^{-3/2}$ in the mean number of atoms per lattice site $\bar{n}$, and standard quantum limit (SQL) scaling $M^{1/2}$ in the number of lattice sites M. In contrast, we find that the optimal scaling from conventional collapse-and-revival dynamics, which do not exploit entanglement of motional and spin degrees of freedom, is $\bar{n}^{-3/4}$. Our analysis requires $M \gg 1$ and for realistic lattice systems $\bar{n} \lesssim 5$; consequently, the scaling in total atom number $N = M\bar{n}$ is below the Heisenberg bound. Nevertheless, we find that measurements testing the predicted scaling behaviors for interaction-based metrologies should be possible in a lattice system using quadrature measurements. We note that measuring the quadratures of nonequilibrium lattice fields, our first goal, is less experimentally demanding than determining interaction strengths with optimal precision. Recently, super-Heisenberg scaling has been realized in another system [20].

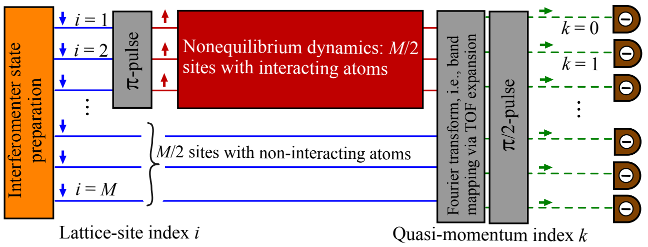
Interferometer state preparation
$i=1$
$i=2$
$i=M$
π-pulse
Nonequilibrium dynamics: M/2 sites with interacting atoms
M/2 sites with non-interacting atoms
Fourier transform, i.e., band mapping via TOF expansion
π/2-pulse
$k=0$
$k=1$
Lattice-site index i
Quasi-momentum index k

FIG. 1: (Color online) Schematic of quadrature operator interferometer for two-state atoms held in M optical lattice sites. Time evolution is left to right. The left-most box represents initial state preparation. Solid and dashed lines correspond to atoms in lattice sites i and Bloch states with quasi-momenta k, respectively. Bold-red and thin-blue lines are atoms in spin states $|a\rangle$ and $|b\rangle$, respectively. Green lines indicate superposition states. Arrows specify spin states. Gray and red boxes correspond to unitary operations described in the text. Detectors (brown) at right measure population differences between spin states at quasi-momenta k.

In the following, we first describe the interferometric technique and propose implementations. We next analyze the special case of atoms held in a deep, cubic lattice with negligible tunneling, and obtain analytic predictions for the time evolution of both quadrature observables and their fluctuations. We emphasize, however, that the technique can provide time-resolved quadrature measurements for more complicated Hamiltonians and lattice geometries (e.g., cubic, honeycomb, superlattices [28–31]), including systems with tunneling, spin-orbit couplings using artificial gauge fields [9], and higher-band effects [32–34], and a new method for studying quench dynamics [35–37]. Related theoretical developments on collapse-and-revival physics can be found in [10, 38–40].

Interferometry technique. Figure 1 shows a schematic of the quadrature interferometer. First, a superfluid of two-component bosonic atoms, with spin states $|a\rangle$ and $|b\rangle$, are prepared in an optical lattice with all atoms in state $|b\rangle$. Interactions between b-state atoms (b atoms) are then slowly turned off with a Feshbach resonance, such that the initial interferometer state is a coherent state with $k=0$ quasi-momentum in the lowest Bloch band of an optical lattice potential. We therefore have $|\psi_{k=0}\rangle = \exp(\gamma B^\dagger_{k=0} - \gamma^* B_{k=0})|0\rangle$, where $|0\rangle$ is the empty lattice, B_k annihilates b atoms with quasi-momentum k, and the mean total atom number is $\bar{N} = |\gamma|^2$. We can re-express this as the separable state $|\psi_{k=0}\rangle = \prod_{i=1}^{M} \exp(\beta b_i^\dagger - \beta^* b_i)|0\rangle$, where $B_{k=0} = \sum_i b_i/\sqrt{M}$ and b_i annihilate b atoms in the lowest Wannier function of lattice site i. The mean atom number per lattice site is $\bar{n} = |\beta|^2 = \bar{N}/M$. For notational simplicity, we suppress the band index and vectorial nature of i and k. As an aside, assuming an initial Fock state $\left(B^\dagger_{k=0}\right)^N|0\rangle/\sqrt{N!}$ (e.g., see [41]) leads to the same interferometer results found below with finite-size corrections of order $M^{-3/2}$.

The lattice depth is next increased to turn off tunneling without exciting atoms to higher bands, and the Wannier function can be approximated by the energetically-lowest local orbital in a site. At this point atoms neither tunnel nor interact. A π-pulse between internal states a and b is then applied to half of the lattice sites, transforming the system state to $\prod_{i=1}^{M/2} \exp(\beta a_i^\dagger - \beta^* a_i) \otimes \prod_{j=M/2+1}^{M} \exp(\beta b_j^\dagger - \beta^* b_j)|0\rangle$, where a_i annihilates a state atoms (a atoms) in the lowest orbital of site i. The π-pulse is the first beam splitter of the interferometer, creating two arms with a and b atoms, respectively.

After the π-pulse, atoms are held for a variable evolution time t. The a atoms interact and undergo nonequilibrium dynamics, while use of the Feshbach resonance ensures that b atoms remain non-interacting and provide a well-characterized reference "beam" state. Spatial separation between a and b atoms is required because it effectively turns off their mutual interactions. After this point, we can change the system dynamics to a "nontrivial" Hamiltonian, as long spatial separation of a and b atoms is maintained. For example, tunneling can be turned back on, the lattice geometry dynamically transformed, or external fields applied.

The second beam splitter combines two operations. First, a Fourier transform on atom spatial modes is applied, transforming site indices i into quasi-momentum indices k. This is achieved by releasing atoms from the lattice followed by (time-of-flight) expansion until all atoms have spatially overlapping wavefunctions. Second, a $\pi/2$-pulse with tunable phase χ is applied to the internal states of all atoms, driving $|a\rangle \to (e^{i\chi/2}|a\rangle + e^{-i\chi/2}|b\rangle)/\sqrt{2}$ and $|b\rangle \to (-e^{i\chi/2}|a\rangle + e^{-i\chi/2}|b\rangle)/\sqrt{2}$.

Finally, we measure the observable $S_k = A_k^\dagger A_k - B_k^\dagger B_k$ by detecting the difference between the number of a and b atoms in quasi-momentum k *after* the second beam splitter. Switching to the Heisenberg picture and using $A_k \to (e^{i\chi/2} A_k + e^{-i\chi/2} B_k)/\sqrt{2}$ and $B_k \to (-e^{i\chi/2} A_k + e^{-i\chi/2} B_k)/\sqrt{2}$ at the second beam splitter, we find that the observable is equivalent to $S_k = A_k^\dagger B_k e^{-i\chi} + B_k^\dagger A_k e^{i\chi}$ with expectation values taken with respect to wavefunctions just *before* the second beam splitter.

Because the many-body wavefunction is separable in the internal atomic states before the $\pi/2$-pulse, it follows that $\langle S_k\rangle = \langle A_k\rangle\langle B_k^\dagger\rangle e^{-i\chi} + \langle A_k^\dagger\rangle\langle B_k\rangle e^{i\chi}$. The non-interacting reference atoms give $\langle B_k\rangle = \beta g_k$ with $\beta = \sqrt{\bar{n}} e^{i\theta}$ and the complex-valued g_k depends only on lattice geometry and distribution of b atoms. In particular, $g_{k=0} = \sqrt{M}/2$ for any lattice geometry and atom distribution. We therefore find

$$\langle S_k\rangle = 2\sqrt{\bar{n}}|g_k|\langle X_k\rangle, \tag{1}$$

where X_k is the quadrature observable with tunable phase $\zeta_k = \arg(e^{i(\theta+\chi)} g_k)$. In contrast, regular collapse-and-revival experiments [4, 12, 14, 42], using atoms in only one spin state, measure the quasi-momentum distribution $R_k = A_k^\dagger A_k$.

Implementations. Realization of the interferometer requires two internal atomic states that have little or no two-body collisional loss, while allowing for tuning of $b + b$ collisions to turn off interactions. We suggest the two energetically-lowest hyperfine states of bosonic alkali-metal atoms as only weak magnetic dipole-dipole and second-order spin-orbit interactions can cause inelastic loss. Candidates are ^{87}Rb near the narrow resonance at a magnetic field B of 100.7 mT [43] and ^{39}K near a much broader resonance at 40.2 mT [44], the latter requiring less stringent field control. Other examples can be found in [27]. Figure 2a shows the scattering length a_s of the ^{39}K resonance as a function of B and indicates two field values where one of the two hyperfine states has zero scattering length and, hence, does not interact.

The initial state of the interferometer is prepared by starting with a (superfluid) Bose condensate of *interacting* b-state atoms in a weak trap with level spacing $\hbar\omega_{\rm w}$, typically harmonic with $\omega_{\rm w}/2\pi = 1$ Hz-100 Hz; $\hbar$ is Planck's reduced constant. After adiabatically turning on the optical lattice, the system can be described by the single-band Bose-Hubbard Hamiltonian [45–48] with tunneling energy J and atom-atom interaction strength U_{bb} proportional to a_s. In a simple cubic lattice, a superfluid ground state requires $J \gg U_{bb}/(5.83 \times 6)$ at the end of the adiabatic ramp (the numerical factor follows from a 3D mean-field calculation). Typically, $U_{bb}/h \sim 1$ kHz away from Feshbach resonances. Due to atom-atom interactions, at this stage the superfluid is only an approximate coherent state.

Figure 2b shows the next step in initial state preparation. Slowly turning off U_{bb} at fixed J using a Feshbach resonance over timescale $\tau_{\rm int}$, the ground state approaches the desired coherent state of non-interacting b atoms. Choosing $\tau_{\rm int} \gg 2\pi/\omega_{\rm w}$ minimizes excitation from zero quasi-momentum. After interactions are ramped-off, tunneling is suppressed by increasing lattice depth with time scale $\tau_{\rm tun}$. Choosing $\tau_{\rm tun} \ll 2\pi/\omega_{\rm bg}$, where $\hbar\omega_{\rm bg}$ is the lattice band gap (typically $\omega_{\rm bg}/2\pi = 10$ kHz-100 kHz), suppresses excitation to higher bands.

The first beam splitter, a spatially selective π-pulse, can be implemented, for example, by illuminating only the top half of the lattice sites (see Fig. 2c) with lasers driving optical Raman transitions via off-resonant transitions to electronically-excited states. The interaction strength for a atoms is U_{aa}. This approach is limited by the boundary over which the Raman laser intensities go to zero, which is no sharper than the laser wavelength. Uncertainty in the fraction of a versus b atoms leads to only small corrections of order $M^{-3/2}$. An alternative approach uses dynamically transformable lattices while simultaneously flipping selected spin states. For example, Refs. [13, 42] used spin-dependent lattices to transform from a single- to double-well lattice where the spin state of atoms alternates with lattice site. In principle, alternating planes of a and b atoms can be created (see Fig. 2d) and our interferometric techniques used to study correlations in two-dimensional many-body physics.

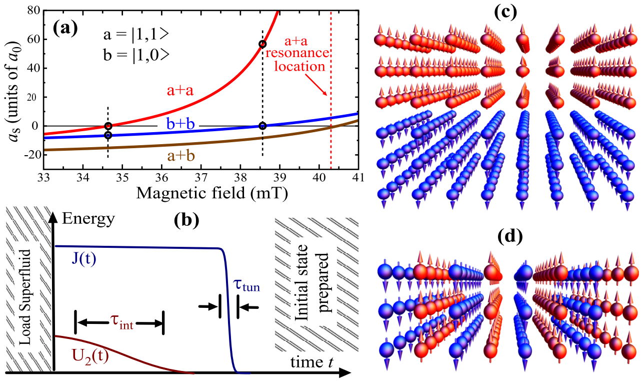

FIG. 2: (Color Online) (a) Scattering lengths a_s of ^{39}K collisions versus magnetic field B near a Feshbach resonance located at $B \approx 40$ mT. Curves are labeled by $|fm\rangle = |11\rangle$ and $|10\rangle$, the energetically lowest hyperfine channels of ^{39}K. Two operating points for the interferometer are shown by black-dotted lines. (Here $1a_0 = 0.0529$ nm). (b) The interferometer initial state, a coherent state of non-interacting atoms, is created starting from a superfluid of interacting atoms by using a Feshbach resonance to slowly turn off the interaction strength U_{bb}, followed by faster turn off of the tunneling rate J. See text for time and energy scales. Panels (c) and (d) show two possible atom distributions after the site-specific π-pulse. In panel (c) atoms in state a (red spheres) and b (blue spheres) are located in the top and bottom half, respectively. In panel (d) planes of state a and b atoms alternate.

The second beam splitter involves release and expansion from the lattice followed by a global $\pi/2$ pulse on the internal state of all atoms. The latter operation requires no spatial selectivity and can be implemented with Raman transitions, or microwave and radio-frequency radiation. The phases $\pi/2$ and χ are controllable by choosing the polarization of the radiation relative to the applied magnetic field; the required techniques have been demonstrated in atomic clock and ion trap quantum computing implementations [49]. Requirements on expansion time are analyzed in [50], and we estimate that ~ 20 ms is sufficient for operation of the interferometer.

Finally, there are corrections due to interactions after atoms are released from the lattice. Following [50], we model the dominant effect by a time-varying U_{aa} proportional to the inverse volume of the expanding local orbital. This leads to a small additional evolution time of order $1/\omega_{\rm bg}$, typically ~ 10 μs, and independent of hold time t. Corrections due to interactions between atoms originating from different lattice sites are even smaller because of negligible overlap of their wavefunctions immediately after release. To minimize corrections to the a atom reference state and unwanted interactions between a and b atoms, the $\pi/2$ pulse should be delayed $\gtrsim 1/\omega_{\rm bg}$, but applied before significant phase shifts from magnetic field inhomogeneities arise. Effects of field gradients after the $\pi/2$ pulse only lead to shifts in the relative location of the $k = 0$ modes for a- and b-atom clouds.

Nonequilibrium dynamics. The factorization property leading to Eq. 1 holds even if tunneling and other modified dynamics are induced for the interacting a atoms after the first beam splitter, making it possible to use the technique to measure the quadrature of nonequilibrium fields for many types of Hamiltonians (e.g. systems with spin-orbit couplings, different lattice geometries, or applied fields). Below, we analyze the interferometer and predict the quadrature evolution for the relatively simple evolution of the Bose-Hubbard model without tunneling, i.e. $H_{\mathrm{MB}} = (U_{aa}/2)\sum_{i=1}^{M/2} a_i^\dagger a_i^\dagger a_i a_i$. Effective multibody interactions [51–53] are omitted for simplicity.

We focus on the normalized $k = 0$ quasi-momentum observable $s_0(t) = \langle S_{k=0}(t)\rangle/\bar{N}$, which is proportional to the order parameter. (For other Hamiltonians $k \neq 0$ quasi-momenta may be interesting.) Defining single-site quadrature operators $x_i = (e^{-i\zeta_0}a_i + e^{i\zeta_0}a_i^\dagger)/2$, we find $s_0(t) = \langle x_i(t)\rangle/(2\sqrt{\bar{n}})$, after expanding the momentum operator in terms of site operators and realizing that the time evolution is the same for all sites. For H_{MB} we derive $\langle x_i(t)\rangle = \sqrt{\bar{n}}\exp([\cos(\phi) - 1]\bar{n})\cos(\bar{n}\sin(\phi) + \zeta_0)$, with phase $\phi = U_{aa}t/\hbar$. Figures 3a and b show examples of the periodic evolution of $\langle x_i(t)\rangle/\sqrt{\bar{n}}$ for several values of ζ_0 and $\bar{n}$. The interferometer makes possible direct experimental verification of these quadrature dynamics. The time evolution of $\mathcal{R}_{k=0}/\bar{N} = |\langle a_i\rangle|^2/\bar{n}$ (assuming large M), determined by regular collapse-and-revival measurements [4, 12–14], is also shown.

The fluctuations in quadratures observable for nonequilibrium Bose gases in deep lattices are also interesting. Figures 3c and d shows the analytic time-dependent (single-site) uncertainty $\sigma_{xi} = \langle(x_i - \langle x_i\rangle)^2\rangle^{1/2}$ as a function of time. For a coherent state for any $\bar{n}$ and ζ_0, $\sigma_{xi} = 1/2$, corresponding to the SQL and shown by horizontal dashed lines; $\sigma_{xi} < 1/2$ indicates quadrature squeezing. For most times and phases ζ_0, the uncertainty is $\sigma_{xi} > 1/2$; in fact, a "plateau" develops for large $\bar{n}$ where σ_{xi} approaches $\sqrt{2\bar{n}+1}/2$. For times near integer multiples of $U_{aa}t/h$ and values of ζ_0 near zero, however, $\sigma_{xi} < 1/2$, and the fluctuations in $\langle x_i\rangle$ are reduced below the SQL. This is seen in Fig. 3c for $\zeta_0 = 0$, where we find that the minimum value of σ_{xi} approaches a constant ≈ 0.29 for large $\bar{n}$. In contrast, Fig. 3d shows that σ_{xi} for $\zeta_0 = \pi/2$ is always antisqueezed.

Interaction-based metrology. In addition to directly measuring field quadratures, the interferometry can be used to measure interaction strengths, although achieving optimal performance is experimentally more demanding. The period h/U_{aa}, and hence U_{aa}, can be obtained by determining times t_1 and $t_2 > t_1$ at which $s_0(t)$ and its time derivative are the same. Figure 3a shows an example where $U_{aa} = h/(t_2 - t_1)$. Error propagation gives the fractional uncertainty

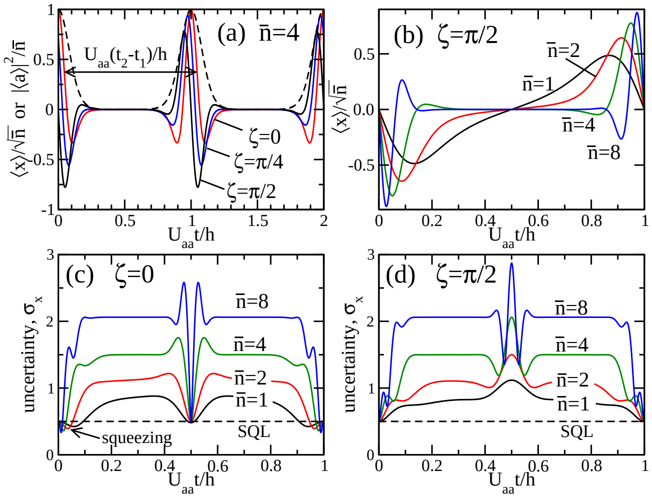

FIG. 3: (Color online) Panels (a) and (b) show the normalized single-site quadrature $\langle x_i\rangle/\sqrt{\bar{n}}$ (solid lines) as a function of evolution time in units of h/U_{aa} for various quadrature phases and mean atom number $\bar{n}$. The double-sided arrow indicates a possible time interval for measuring U_{aa}. The density operator $|\langle a_i\rangle|^2/\bar{n}$ (dashed line) is only shown for $\bar{n} = 4$. Panels (c) and (d) show the quadrature uncertainties σ_{xi} as a function of evolution time and $\bar{n}$, for $\zeta_0 = 0$ and $\zeta_0 = \pi/2$, respectively. The dash-dotted line, labeled SQL, indicates $\sigma_{xi} = 1/2$ for a coherent state.

$$\frac{\delta U_{aa}}{U_{aa}} = \frac{\sqrt{2}}{\pi\sqrt{M/2}}\left|\frac{1}{d\langle x_i\rangle/d\phi}\right|\sqrt{\sigma_{xi}^2 + \frac{\langle x_i\rangle^2}{2\bar{n}}}\,, \qquad (2)$$

with expectation values evaluated at phase $\phi_1 = U_{aa}t_1/\hbar$, assuming equal contributions at t_1 and t_2 added in quadrature. The fractional uncertainty gives SQL scaling $\propto 1/\sqrt{M/2}$ in number of a-atom lattice sites, as expected for a site-separable wavefunction, and we can view the interferometer as $M/2$ independent probes of $\bar{n}$ interacting atoms. The second term under the square root is due to the uncertainty in total atom number $\bar{N}$. The uncertainty also scales as $1/m$ in the number of oscillation periods m; for brevity we set $m = 1$.

Minimizing $\delta U_{aa}/U_{aa}$ based on measurements of $x_i(t)$ involves a trade-off between identifying optimal measurement times t_1, t_2 (or phases ϕ_1, ϕ_2) that maximize the slope $d\langle x_i\rangle/d\phi$ while minimizing σ_{xi}. We find that the smallest (optimal) fractional uncertainty

$$(\delta U_{aa}/U_{aa})_{\mathrm{quad}} = (1/2\pi)M^{-1/2}\bar{n}^{-3/2}, \qquad (3)$$

is obtained from the quadrature observable with $\zeta_0 = \pi/2$, and measurements made when $\langle x_i\rangle = 0$ and the slope $d\langle x_i\rangle/d\phi$ is maximum. This occurs at phases $\phi_1 = 0$ and $\phi_2 = 2\pi$, corresponding to times $t_1 = 0$ and $t_2 = 2\pi\hbar/U_{aa}$. Because $\langle x_i\rangle = 0$ and $\sigma_{xi} = 1/2$ at these times, the result is independent of uncertainty in $\bar{N}$. For other ζ_0, the numerical prefactor in Eq. (3) is larger, but the scaling in $\bar{n}$ is the same. As noted in *Implementations*, the small correction from interactions during expansion can be included in the determination of $t_{1,2}$.

At optimal measurement times the state is unsqueezed, and the super-Heisenberg scaling $\bar{n}^{-3/2}$ derives from the nonlinear dependence of $d\langle x_i\rangle/d\phi$ on $\bar{n}$. Our quadrature interferometer yields the best possible scaling behavior predicted for interaction-based metrology schemes based on two-body interactions and non-entangled states [16]. We have also analyzed the minimal uncertainty possible from conventional collapse and revival measurements of $\langle\mathcal{R}_{k=0}(t)\rangle/\bar{N}$. We obtain the analytic estimate $(\delta U_{aa}/U_{aa})_{\rm conv} = (2/3)^{3/4}\pi^{-1}M^{-1/2}\bar{n}^{-3/4}$, and have confirmed it is in good agreement with numerical evaluation. The scaling is significantly less advantageous than what is possible using the quadrature interferometry.

We can compare our predictions with conventional collapse-and-revival experiments. Will *et al.* [12] obtained $\delta U_{aa}/U_{aa} \approx 2\times10^{-2}$ with $\bar{N} = 2\times10^{5}$ atoms and $\bar{n} = 2.5$. For these parameters $(\delta U_{aa}/U_{aa})_{\rm conv} = 3\times10^{-4}$. The larger experimental uncertainty is likely due to fluctuations in the total atom number and lattice-laser intensities. For the quadrature interferometer $(\delta U_{aa}/U_{aa})_{\rm quad} = 1.2\times10^{-4}$ is, in principle, possible, giving nearly a factor of three improvement even with $\bar{n} = 2.5$. As noted above, we also predict less sensitivity to fluctuations in $\bar{N}$ using the quadrature technique.

Outlook. Our analysis suggests that even for small (realistic) $\bar{n}$ it should be possible to test predicted scaling behaviors for interaction-based metrologies in an optical lattice system. There are many interesting directions for future research. For example, are there interferometer states that give $\bar{n}^{-2}$ scaling per lattice site, as suggested by the analysis in [16]? Are there implementations where interesting information lies in $k \neq 0$ quasi-momenta states? Can we modify the interferometer to measure observables such as $\langle a_i a_j\rangle$, and use entanglement between atoms in different sites to measure nonlocal field correlations? There are also practical challenges facing implementations, including the effects of inhomogeneities, lattice (laser) fluctuations, and limits on both atom number per site and total atom number. Even with non-optimal measurements, however, the interferometer technique developed here should expand the toolkit for studying nonequilibrium dynamics in optical lattices.

PRJ and ET acknowledge support from the US Army Research Office under contract/grant 60661PH. PRJ also acknowledges computing resources provided by the American University High Performance Computing System. ET acknowledges support from a NSF Physics Frontier Center. Finally, we thank Khan Mahmud, Lei Jiang, and Nathan Harshman for valuable discussions.

[1] M. Lewenstein, A. Sanpera, V. Ahufinger, B. Damski, A. Sen, and U. Sen, Adv. Phys. **56**, 243 (2007).

[2] D. Jaksch and P. Zoller, Ann. Phys. **315**, 52 (2005).

[3] I. Bloch, J. Dalibard, and S. Nascimbène, Nat. Phys. **8**, 267 (2012).

[4] M. Greiner, O. Mandel, T. W. Hänsch, and I. Bloch, Nature **419**, 5154 (2002).

[5] R. Schützhold, M. Uhlmann, Y. Xu, and U. R. Fischer, Phys. Rev. Lett. **97**, 200601 (2006).

[6] U. R. Fischer and R. Schützhold, Phys. Rev. A **78**, 061603 (2008).

[7] S. E. Pollack, D. Dries, R. G. Hulet, K. M. F. Magalhães, E. A. L. Henn, E. R. F. Ramos, M. A. Caracanhas, and V. S. Bagnato, Phys. Rev. A **81**, 053627 (2010).

[8] J. Simon, W. S. Bakr, R. Ma, M. E. Tai, P. M. Preiss, and M. Greiner, Nature **472**, 307 (2011).

[9] Y.-J. Lin, K. Jiménez-García, and I. B. Spielman, Nature **471**, 83 (2011).

[10] A. J. Daley, H. Pichler, J. Schachenmayer, and P. Zoller, Phys. Rev. Lett. **109**, 020505 (2012).

[11] C.-L. Hung, V. Gurarie, and C. Chin, arXiv:1209.0011 (2012).

[12] S. Will, T. Best, U. Schneider, L. Hackermuller, D.-S. Luhmann, and I. Bloch, Nature **465**, 197 (2010).

[13] M. Anderlini, J. Sebby-Strabley, J. Kruse, J. V. Porto, and W. D. Phillips, J. Phys. B **39**, S199 (2006).

[14] J. Sebby-Strabley, B. L. Brown, M. Anderlini, P. J. Lee, W. D. Phillips, J. V. Porto, and P. R. Johnson, Phys. Rev. Lett. **98**, 200405 (2007).

[15] S. Boixo, S. T. Flammia, C. M. Caves, and J. M. Geremia, Phys. Rev. Let. **98**, 090401 (2007).

[16] S. Boixo, A. Datta, M. J. Davis, S. T. Flammia, A. Shaji, and C. M. Caves, Phys. Rev. Lett. **101**, 040403 (2008).

[17] S. Choi and B. Sundaram, Phys. Rev. A **77**, 053613 (2008).

[18] Y. C. Liu, G. R. Jin, and L. You, Phys. Rev. A **82**, 045601 (2010).

[19] J. Grond, U. Hohenester, J. Schmiedmayer, and A. Smerzi, Phys. Rev. A **84**, 023619 (2011).

[20] M. Napolitano, M. Koschorreck, B. Dubost, N. Behbood, R. J. Sewell, and M. W. Mitchell, Nature **471**, 486 (2011).

[21] V. Giovannetti, S. Lloyd, and L. Maccone, Nat. Photon. **5**, 222 (2011).

[22] J. Javanainen and H. Chen, Phys. Rev. A **85**, 063605 (2012).

[23] D. F. Walls and G. J. Milburn, *Quantum Optics* (Springer Berlin/Heidelberg, 2008), 2nd ed.

[24] T. Kitagawa, A. Aspect, M. Greiner, and E. Demler, Phys. Rev. Lett. **106**, 115302 (2011).

[25] C. J. Pethick and H. Smith, *Bose-Einstein Condensation in Dilute Gases* (Cambridge University Press, 2008), 2nd ed.

[26] L. Pitaevskii and S. Stringari, *Bose-Einstein Condensation* (Oxford University Press, 2003), 1st ed.

[27] C. Chin, R. Grimm, P. Julienne, and E. Tiesinga, Rev. Mod. Phys. **82**, 1225 (2010).

[28] J. Sebby-Strabley, M. Anderlini, P. S. Jessen, and J. V. Porto, Phys. Rev. A **73**, 033605 (2006).

[29] B. Vaucher, A. Nunnenkamp, and D. Jaksch, New J. Phys. **10**, 023005 (2008).

[30] P. Barmettler, A. M. Rey, E. Demler, M. D. Lukin,

I. Bloch, and V. Gritsev, Phys. Rev. A **78**, 012330 (2008).

[31] S. Al-Assam, R. A. Williams, and C. J. Foot, Phys. Rev. A **82**, 021604 (2010).

[32] T. Müller, S. Fölling, A. Widera, and I. Bloch, Phys. Rev. Lett. **99**, 200405 (2007).

[33] W. S. Bakr, A. Peng, M. E. Tai, R. Ma, J. Simon, J. I. Gillen, S. Flling, L. Pollet, and M. Greiner, Science **329**, 547 (2010).

[34] P. Soltan-Panahi, D.-S. Lühmann, J. Struck, P. Windpassinger, and K. Sengstock, Nat. Phys. **8**, 71 (2012).

[35] W. H. Zurek, U. Dorner, and P. Zoller, Phys. Rev. Lett. **95**, 105701 (2005).

[36] F. M. Cucchietti, B. Damski, J. Dziarmaga, and W. H. Zurek, Phys. Rev. A **75**, 023603 (2007).

[37] D. Chen, M. White, C. Borries, and B. DeMarco, Phys. Rev. Lett. **106**, 235304 (2011).

[38] M. Buchhold, U. Bissbort, S. Will, and W. Hofstetter, Phys. Rev. A **84**, 023631 (2011).

[39] U. R. Fischer and B. Xiong, Europhys. Lett. **99**, 66003 (2012).

[40] C. Gramsch and M. Rigol, Phys. Rev. A **86**, 053615 (2012).

[41] J. Schachenmayer, A. J. Daley, and P. Zoller, Phys. Rev. A **83**, 043614 (2011).

[42] M. Anderlini, P. J. Lee, B. L. Brown, J. Sebby-Strabley, W. D. Phillips, and J. V. Porto, Nature **448**, 452 (2007).

[43] A. Marte, T. Volz, J. Schuster, S. Durr, G. Rempe, E. G. M. van Kempen, and B. J. Verhaar, Phys. Rev. Lett. **89**, 283202 (2002).

[44] C. D'Errico, M. Zaccanti, M. Fattori, G. Roati, M. Inguscio, G. Modugno, and A. Simoni, New J. Phys. **9**, 223 (2007).

[45] M. P. A. Fisher, P. B. Weichman, G. Grinstein, and D. S. Fisher, Phys. Rev. B **40**, 546 (1989).

[46] J. K. Freericks and H. Monien, Europhys. Lett. **26**, 545 (1994).

[47] D. Jaksch, C. Bruder, J. I. Cirac, C. W. Gardiner, and P. Zoller, Phys. Rev. Lett. **81**, 3108 (1998).

[48] D. van Oosten, P. van der Straten, and H. T. C. Stoof, Phys. Rev. A **63**, 053601 (2001).

[49] H. Häffner, C. Roos, and R. Blatt, Phys. Rep. **469**, 155 (2008).

[50] E. Toth, A. M. Rey, and P. B. Blakie, Phys. Rev. A **78**, 013627 (2008).

[51] P. R. Johnson, E. Tiesinga, J. V. Porto, and C. J. Williams, New J. Phys. **11**, 093022 (2009).

[52] P. R. Johnson, D. Blume, X. Y. Yin, W. F. Flynn, and E. Tiesinga, New J. Phys. **14**, 053037 (2012).

[53] U. Bissbort, F. Deuretzbacher, and W. Hofstetter, Phys. Rev. A **86**, 023617 (2012).